European Journal of Medicinal Chemistry 46 (2011) 129–136

Contents lists available at ScienceDirect

European Journal of Medicinal Chemistry

journal homepage: http://www.elsevier.com/locate/ejmech

Original article

Isoxazolidinyl polycyclic aromatic hydrocarbons as DNA-intercalating antitumor agents

Antonio Rescifina [a,*], Ugo Chiacchio [a], Antonino Corsaro [a], Anna Piperno [b], Roberto Romeo [b]

[a] Dipartimento di Scienze Chimiche, Università di Catania, Viale Andrea Doria 6, Catania 95125, Italy
[b] Dipartimento Farmaco-Chimico, Università di Messina, Via SS. Annunziata, Messina 98168, Italy

ARTICLE INFO

Article history:
Received 6 August 2010
Received in revised form
20 October 2010
Accepted 21 October 2010
Available online 28 October 2010

Keywords:
DNA intercalation
Antitumor agent
Docking
Polycyclic aromatic hydrocarbon
Isoxazolidine
1,3-Dipolar cycloaddition

ABSTRACT

The second generation and an isosteric series of isoxazolidinyl polycyclic aromatic hydrocarbons, as DNA-intercalator agents designed to act on remotely implanted tumors, have been synthesized in good yields according to the 1,3-dipolar cycloaddition methodology. The structure of the obtained cycloadducts has been determined by NOE experiments and supported by computational studies at PM3 level. The utility of this new template in the synthesis of structures designed to capitalize on its intercalative properties has been examined. All the obtained compounds have been tested for their in vitro cytotoxic activity and the most potent of them showed an IC_{50} of 9 μM upon the human lung cancer (A-549) cell and a binding constant, for the intercalation with calf thymus DNA, of 9.6×10^4 M^{-1}. Biological and docking studies showed that these compounds complex exclusively by intercalation between base pairs, approaching the DNA from its minor groove, with a neat selectivity for the AT or GC nucleobases.

1. Introduction

The best described mode for the reversible binding of small molecules to DNA is represented by their intercalation between the base pairs, firstly described by Lerman for the acridine proflavine [1] (Fig. 1). Intercalation is the preferred binding mode of virtually flat polyaromatic ligands of sufficiently large surface area and suitable steric properties. The driving forces for intercalation are primarily stacking interactions between the ligand chromophore and the base pairs, with entropic factors of significant, but lesser and variable importance [2].

The size and nature of the intercalating chromophore [3] is determinant for the binding mode and a number of studies suggest that fused two-ring systems, i.e., naphthalene-type, are the minimum necessary for an effective intercalation [4]. Moreover, NMR shift and line width changes indicate that two-ring naphthalene-type ligands intercalate only if they possess pendent cationic side chain, and have similar affinities irrespective of the presence of charged or uncharged nitrogen atoms in the aromatic system. In contrast, fused three-ring systems such as acridines have sufficient stacking interactions to intercalate without the need for appended side chains.

Although structure–activity relationship studies have demonstrated a positive relationship between the DNA binding strength of intercalating agents and biological potency, in both in vivo and in vitro leukemia models [5], this relationship did not hold for activity against remotely implanted solid tumors [6] where drug distribution properties may be much more important. In fact, the biological activity also appears to be linked to the binding kinetics of intercalating agents to DNA, with longer average residence time of a ligand at a particular binding site correlating positively with the biological potency.

A high DNA binding affinity correlates positively with in vitro cytotoxicity for several series of DNA-intercalating agents, but this property is also thought to be the factor limiting the penetration of such drugs into multicellular spheroids which are used as models of solid tumor.

Such effects of DNA binding on the drug diffusion have been shown in tumor spheroids, with tightly binding compounds, such as doxorubicin, mitoxantrone and the anthrapyrazole AP-10 (Fig. 1), distributing poorly [7]. Experiments using multicellular layers of defined geometry growing on porous Teflon supports also showed that less tightly binding compounds have higher rates of flux, which is attributed to higher free drug diffusion coefficients [8].

According to these considerations, many efforts have been developed to find compounds with an intercalative binding mode of action, but with a minimum of DNA binding strength. This is

* Corresponding author. Tel.: +39 095 738 50 14; fax: +39 06 233 208 980.
E-mail address: arescifina@unict.it (A. Rescifina).

0223-5234/$ – see front matter © 2010 Elsevier Masson SAS. All rights reserved.
doi:10.1016/j.ejmech.2010.10.023

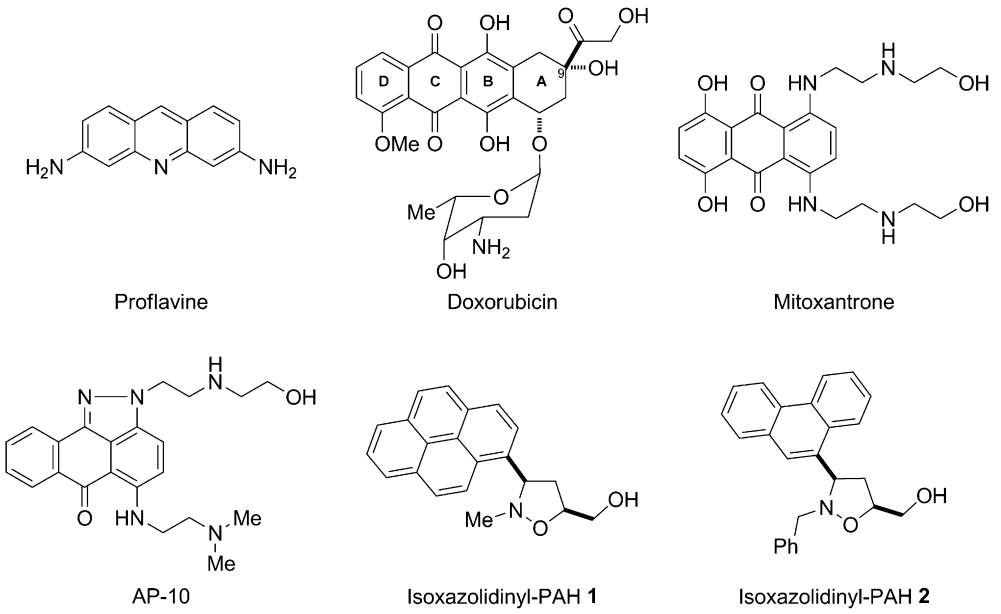

Fig. 1. Selected DNA-intercalating agents.

what Danny and coworkers have defined as "minimal intercalator", a concept proposed to incorporate the requirements of a mandatory intercalative binding mode together with the lowest possible level of binding [9].

For drugs that bind to DNA, the effective diffusion coefficient (D_{eff}) that determines the rate of extra vascular diffusion, is greatly lowered by DNA binding, in direct proportion with the binding constant. It is given by $D_{eff} = D/(1 + K_{DNA}S_f)$, where D is the diffusion coefficient, K_{DNA} is the DNA association constant and S_f is the concentration of available DNA binding sites [10]. Assuming a total DNA binding site concentration of about 1 mM for a binder of low sequence specificity (about 10% of the sites in chromatin), the upper limit of K_{DNA} to keep the diffusion time reasonably rapid on the pharmacological timescale is about 10^4 M^{-1}, suggesting that quite moderate levels of DNA binding can limit diffusion.

Recently, we have synthesized a series of non-ionic isoxazolidinyl polycyclic aromatic hydrocarbons (PAHs) that showed moderate DNA intercalative and cytotoxicity properties [11]. In particular, the pyrenyl- (**1**) and phenanthryl-isoxazolidine (**2**) derivatives, with an IC_{50} of 112 and 78 μM, respectively, on Molt-3 cell line, exhibited promising cytotoxic and apoptotic properties. In light of this, we considered it of importance to shed light into the interaction of **1** with DNA [12]. From these studies emerged that compound **1** binds calf thymus DNA with a binding constant of 6.8×10^3 M^{-1}, and preferentially intercalate in AT reach regions penetrating from the major groove.

On the basis of our continuous interest on this area and with the aim to create new DNA-intercalators possessing the binding constants in the range 10^4–10^5 M^{-1}, in order to easily diffuse targeting remotely implanted tumors, we report in this paper the synthesis, the biological activity and the intercalative binding investigations of isoxazolidinyl-PAHs **6**, **7** and **8**, **9**, the second generation and an isosteric series, respectively, of potential DNA-intercalators, featuring the presence of an imido or amino group linked to isoxazolidine ring on the aromatic planar system of phenanthrene and pyrene nucleus.

Our design is supported by the consideration that the presence of a succinimido group or of a primary, at physiological pH, alkyl ammonium one (pK_a = 9.6 and 10.6, respectively) into the isoxazolidine ring could play an important role in the DNA-recognizing region because of its ability to form favorable intermolecular hydrogen bonds [13] with the DNA backbone, which could contribute to the formation of more stable complexes with respect to the precedent series of isoxazolidinyl-PAH **1** and **2**, and then to a better interaction with DNA sites.

2. Results and discussion

2.1. Chemistry

The cycloaddition of nitrones **3** [11], with *t*-butyl-*N*-allylcarbamate or maleimide, in dry toluene and in a sealed tube at 120 °C for 6 d or 18 h, respectively, using a 1:1.5 relative ratio of dipole to dipolarophile, afforded a mixture of two isoxazolidines **4**, **5**, and **6**, **7** (Scheme 1) in ca. 1.5–4.0:1 ratio (Table 1), with a yield between 80 and 92%.

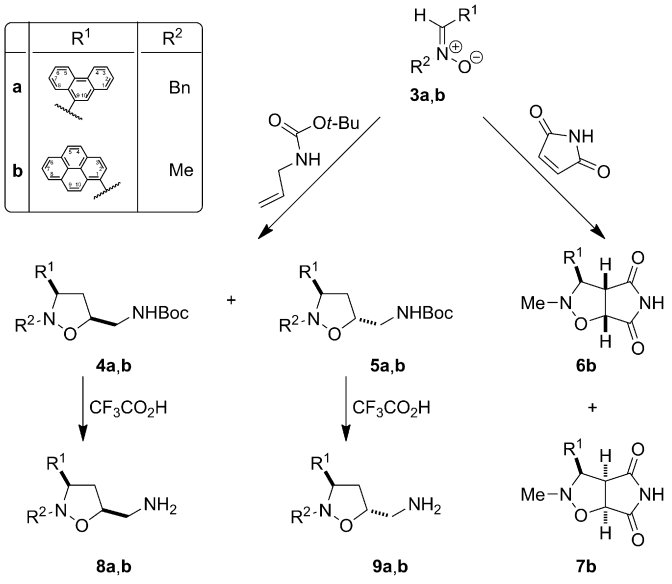

Scheme 1. Synthesis of isoxazolidine-PAHs.

Table 1
Reaction of nitrones **3** with *t*-butyl-*N*-allylcarbamate and maleimide.

Nitrone	R^1	R^2	Dipolarophile	Isolated yield (%)	**4**/**5** and **6**/**7** Ratio
3a	9-phenanthryl	Bn	*t*-Butyl-*N*–allylcarbamate	80	2.0:1
3b	1-pyrenyl	Me	*t*-Butyl-*N*–allylcarbamate	92	1.5:1
3b	1-pyrenyl	Me	Maleimide	87	4.0:1

As reported in Table 1, the investigated reaction was found to be regiospecific, affording a mixture of *cis* and *trans* 5-substituted isoxazolidines **4** and **5** as exclusive adducts. Whereas the isoxazolidines **6** and **7** resulted always *cis*-fused.

All products were purified by preparative centrifuge-accelerated radial thin-layer chromatography (PCAR-TLC) and obtained as pure compounds (see Experimental). The molecular structure of the reaction products was assigned on the basis of analytical and spectroscopic data. The regiochemistry of the cycloaddition process was readily deduced from the ^{1}H NMR measurements. For isoxazolidines **4** and **5**, there was one proton signal at 4.31–4.52 ppm, which corresponded to the H_5 proton; the alternative regioisomers are not reported to show a resonance at this chemical value [14].

The pericyclic reaction showed a low level of *cis*/*trans* stereoselectivity. The reactions with *t*-butyl-*N*-allylcarbamate showed the *cis* isomers **4** as the major products whereas in that with maleimide predominate the *trans* one **6**. The relative stereochemical assignments have been performed by NOE measurements. In particular, in compound **4a** irradiation of H_3 resonance at 4.63 ppm induces a positive NOE effect on the downfield resonance of methylene protons at C_4 (H_{4b}) (5.8%), centered at 3.09 ppm, and on H_5 (0.9%), centered at 4.44 ppm; instead, the irradiation of H_{4a}, centered at 2.04 ppm, not induces any positive NOE on H_3 and H_5 protons. These results indicate that H_3, H_{4b} and H_5 are in a *cis* relationship, as reported in Fig. 2.

Conversely, for *trans* adduct **5a**, a diagnostic NOE effect was observed for H_6 (0.6%) when irradiating the H_3 proton (Fig. 2).

The final desired compounds **8** and **9** were obtained, in high yields (80–95%), upon treatment of their respective precursors, **4** and **5**, with trifluoroacetic acid in dichloromethane at 0 °C for 12–36 h (Scheme 1). In these conditions *cis* isomers completely hydrolyze in 12 h, whereas for the *trans* ones occur 36 h and the conversion not go always to completion.

2.2. Computational stereochemical analysis

The stereochemical outcome of the cycloaddition process can be explained by considering that nitrone **3a** exist exclusively as *Z* isomers whereas nitrone **3b** exist as a mixture of *Z*/*E* (15:1) isomers [11]. PM3 [15] semiempirical calculations give a theoretical support to experimental data; in all the cases the activation enthalpy of the cycloaddition reaction starting from *Z*-nitrones is lower than that of *E*-ones; therefore, we report only the results derived from the reaction of *Z*-nitrones in an *exo* and *endo* mode (Table 2).

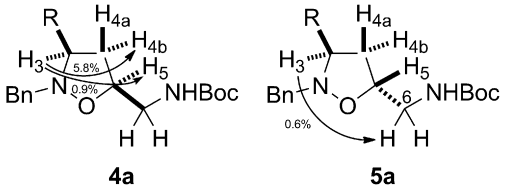

Fig. 2. Selected observed NOEs in compounds **4a** and **5a**.

Table 2
PM3 calculations results on transition state structures for isoxazolidines **4**–**7**.

Compound	ΔH_f *Z-exo* TS	ΔH_f *Z-endo* TS	Calculated ratio **4:5** or **6:7**
4a, **5a**	65.36[a]	65.77	1.99:1
4b, **5b**	52.84	53.10	1.55:1
6b, **7b**	59.15	58.28	4.30:1

[a] All values are in kcal/mol.

The data reported in Table 2 are in satisfactory agreement with the experimental results; the inversion of *cis*/*trans* selectivity, registered for the maleimide adducts, is explainable on the basis of secondary orbital interactions that established between the π-imidic orbitals and the p nitronic nitrogen one in the *Z-endo* approach (Fig. 3).

2.3. Biological evaluation

2.3.1. Cytotoxicity assays

The cytotoxicity of compounds **6**–**9** was evaluated in vitro against human cervical carcinoma (HeLa), human lung cancer (A-549), a panel of leukemia (Molt-3, THP-1) and lymphoma (U-937), as well as against normal African green monkey kidney (Vero) cell lines. As a screening assay, the cytotoxicity was tested using an MTS tetrazolium reduction assay, except for A-549 cell lines, and expressed as IC_{50} values. IC_{50} is the concentration (μM) required to reduce the absorbance values, i.e., the capability of the cells to reduce MTS, by 50% after 20 h of treatment. For A-549 cell lines, the growth inhibition was tested by the sulforhodamine B (SRB) assay [16] where IC_{50} is the drug concentration (μM) that yields 50% less cells than the drug-free control. Results shown in Table 3 indicates that Vero cells were more resistant than tumoral cell lines to the toxicity induced by new synthesized compounds, and that, among the compounds tested, particularly compounds **8b** and **9b** show a high level of cytotoxicity against A-549 cell lines.

In general, the new derivatives **6**, **8** and **9** showed an improved cytotoxic activity over the first template reported by us [11]; but in any case, the actinomycin D, a well-known intercalating agents, possess an extremely higher toxicity with respect to all the new tested compounds. As previously reported [11], the values of IC_{50} of the actinomycin D for lymphoid and monocytoid (Molt-3) cells are less than to 1 μM and an IC_{50} = 11 μM is detected for Vero cell. Literature data [17] reported that at a concentration of 0.5 μg/mL of actinomycin D the number of A-549 cells declined to 40% of the control at 8 h.

Whereas for compounds **8** and **9** the *cis*/*trans* configuration has a weak influence on the cytotoxicity, with the *cis* isomer that is more active of the *trans* one, in the case of the succinimidic

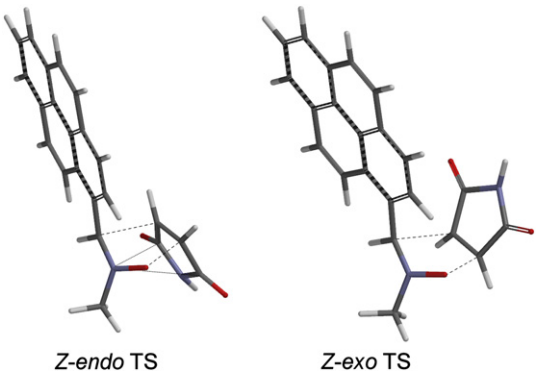

Fig. 3. Transition states for compounds **6b** and **7b**. Broken lines represent C–C and C–O incoming bonds, dotted lines represent secondary orbital interactions.

Table 3
Evaluationof cytotoxicity for compounds **6**–**9** by MTS or SRB assay.[a]

Compound	IC_{50} (μM)					
	HeLa	A-549	Molt-3	THP-1	U-937	Vero
6b	135[b]	83	95	102	130	150
7b	284	328	415	399	>500	>500
8a	50	32	43	55	154	132
8b	15	9	12	19	88	102
9a	45	35	50	61	112	140
9b	15	11	17	18	80	110

[a] Cells were exposed in optimal culture conditions in 96-well plates to five concentrations of the compounds (1, 10, 100, 200, 500 μM) or control medium for 20 h before determining cellular metabolic activity by an MTS tetrazolium compound bioreduction assay or sulforhodamine B assay.
[b] Each value is determined from triplicate samples using a non-linear regression analysis.

derivatives **6** and **7** the *trans* isomer is more reactive. In any case, compound **8b** shows activity on all the tested cell lines and particularly interesting is the cytotoxicity against A-549 cells with an IC_{50} of 9 μM.

2.3.2. DNA binding properties

Compound **8b**, which showed the highest cytotoxicity, was then used as model to investigate the DNA intercalation. So, incubation followed by electrophoretic examination of compound **8b** with ΦX174 RF I DNA showed characteristic streaking of the supercoiled species, indicative of intercalation. Furthermore, in the UV spectral analysis of **8b** and calf thymus DNA, characteristic red shift of 16 nm for DNA were observed on incubation, consistent with intercalation [18]. A titration experiment indicate that the examined compound shows a binding constant, for the intercalation with calf thymus DNA, of 9.6×10^4 M^{-1}, that is 14-fold greater than that with compound **1** ($K_B = 6.8 \times 10^3$ M^{-1}).

2.4. Molecular docking

In order to confirm and rationalize the observed biological results and to get more insight into the intercalation modality, the supramolecular complexes of synthesized compounds with DNA have been investigated by molecular modeling methodology. Moreover, although the obtained compounds are racemates, from a theoretical point of view, and in the perspective to realize the synthesis of enantiomerically pure compounds, a better understanding of the interactions of both stereoisomers will be useful for the rational design of ligands to target specific regions of DNA and for enhanced therapeutic activity. In consideration of this and to test the model, we exploited, at first overtures, the molecular docking of all stereoisomers of compound **1**, knowing its binding constants with poly-d(AT)$_2$ and poly-d(GC)$_2$ ($K_B = 6.0 \times 10^3$ M^{-1} and 1.5×10^3 M^{-1}, respectively) [15].

The adopted molecular modeling template consists of the following three steps: i) poly-d(AT)$_2$ and poly-d(GC)$_2$ were simulated as a dodecamer fragment of (dA–dT)$_2$ and (dG–dC)$_2$, respectively, which were constructed in the B-DNA conformation with the nucleic acids tool, implemented in the HyperChem 7.5 program package [19], and minimized with the Amber96 force field, that is one of the most accurate force fields widely used for proteins and DNA [20]. ii) The simulations of all compounds bound to poly-d(AT)$_2$ and poly-d(GC)$_2$ were carried out, for the intercalation between paired nucleobases, using docking methodology [21]. Firstly, the compound was selected to insert into the middle base-step of each fragment from the minor groove or the major one, respectively. While the compound atom positions fixed, the rest molecules were minimized so as to make the free fragment adjusted to accommodate the ligand suitably. Subsequently the whole system was minimized with a convergence criterion of 0.005 kcal/mol per Å, without any restrains. iii) Finally, we performed a computational automated fine docking on the obtained systems applying the Lamarckian genetic algorithm (LGA) implemented in AutoDock 4.0 [22]. This software has been recently used to accurately reproduce the pose, in the crystallographic structures, of a series of small ligands that bind to nucleic acids, reproducing the binding constants semiquantitatively [23].

Table 4
Calculated binding energies for all stereoisomers of compound **1** intercalated in d(AT)$_2$ and d(GC)$_2$ dodecamers.

Compound **1**	Poly-AT	
	Major groove	Minor groove
3*R*,5*S* (*cis*)	−9.78[a]	−8.63
3*S*,5*R* (*cis*)	−9.44	−9.03
3*R*,5*R* (*trans*)	−9.05	−8.99
3*S*,5*S* (*trans*)	−8.95	−8.92
	Poly-GC	
	Major groove	Minor groove
3*R*,5*S* (*cis*)	−9.24	−9.16
3*S*,5*R* (*cis*)	−9.34	−9.27
3*R*,5*R* (*trans*)	−9.20	−9.01
3*S*,5*S* (*trans*)	−9.37	−9.24

[a] All values are in kcal/mol.

The possibility to achieve complexes by binding along the groove was *a priori* excluded according to previously reported results [12].

The calculated binding energies, ΔG_B, for complexes of all stereoisomers of compound **1** with d(AT)$_2$ and d(GC)$_2$ dodecamer fragments are summarized in Table 4 that points out that the stereoisomer 3*R*,5*S* have the lowest binding energy and clearly prefer the intercalative path from the major groove in the poly-AT fragment, completely in accord with literature [12]. Moreover, its enantiomer (3*S*,5*R*) is just slightly less active, whereas the *trans* ones, that are even less active, showed a net preference for poly-GC fragment, with the intercalation that takes place from the minor groove.

On the base of these results, we chose to study only the isomers with 3*R* configuration and in particular the *cis* ones for compounds **8**. Furthermore, since compounds **8** at the 7.2 physiological pH are monoprotonated, they were studied in this form.

From the inspection of Table 5, that collects the calculated binding energies of the above docking study, it is evident that compound (3*R*,5*S*)-**8b** is the best active one, confirming the biological results, and shows a preference for the poly-AT fragment intercalating from the minor groove. Moreover, the affinity for AT

Table 5
Calculated binding energies for **6**–**8** intercalated in d(AT)$_2$ and d(GC)$_2$ dodecamers.

Compound	Poly-AT	
	Major groove	Minor groove
(3*R*,5*R*)-**6b** (*trans*)	−9.10[a]	−9.70
(3*R*,5*S*)-**7b** (*cis*)	−8.11	−9.12
(3*R*,5*S*)-**8a** (*cis*)	−10.21	−10.69
(3*R*,5*S*)-**8b** (*cis*)	−11.22	−11.35
	Poly-GC	
	Major groove	Minor groove
(3*R*,5*R*)-**6b** (*trans*)	−9.47	−10.21
(3*R*,5*S*)-**7b** (*cis*)	−8.63	−9.34
(3*R*,5*S*)-**8a** (*cis*)	−9.95	−10.42
(3*R*,5*S*)-**8b** (*cis*)	−11.05	−10.30

[a] All values are in kcal/mol.

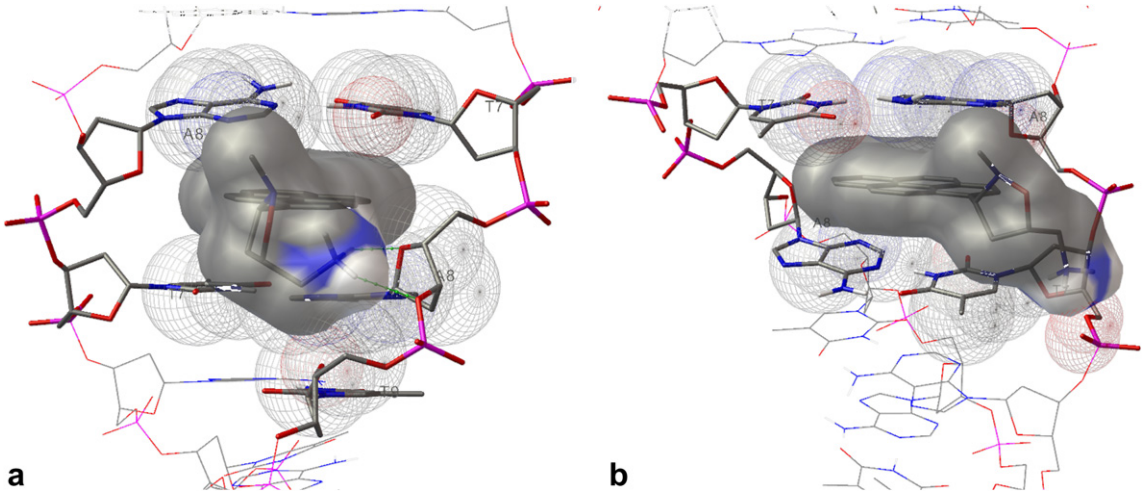

Fig. 4. Plot representing compound 8b intercalated into poly-d(AT)$_2$. (a) From minor groove. (b) From major groove. Dotted lines represents hydrogen bond.

nucleobases is 18-fold greater than that of its precursor (3*R*,5*S*)-**1** ($\Delta\Delta G_{Bind}$ = 1.57 kcal/mol), well in accord with the respective experimental binding constants.

Interestingly, both compounds **6** and **7** showed a marked preference for the GC nucleobases with an insertion from the minor groove.

Fig. 4 reports a plot of compound (3*R*,5*S*)-**8b** intercalated into poly-d(AT)$_2$ from both minor and major grooves; in the minor groove supermolecule is evident the formation of two stabilizing hydrogen bonds between the isoxazolidine ammonium and the O_1 and O_3 atoms of the deoxyribose A8 unit (Fig. 4a). In the case of compound **6**, the best pose shows a hydrogen bond between the isoxazolidinic oxygen and the hydrogen of the G8 guanine 2-amino group.

3. Conclusion

A second generation and an isosteric series of isoxazolidinyl-PAH as DNA-intercalator agents capable to easily diffuse and to act on remotely implanted solid tumors has been synthesized according to the 1,3-dipolar cycloaddition methodology. The utility of this template in the synthesis of structures designed to capitalize on its intercalative properties has been examined.

Compound **8b** shows the better in vitro cytotoxic activity against all tested cell lines, in particular upon the human lung cancer (A-549) cell, and complexes exclusively by intercalation between base pairs, approaching the DNA from its minor groove, with a neat preference for the AT nucleobases. The second generation compounds **6** and **7**, interestingly, showed the highest potency intercalating mostly into the GC nucleobases forthcoming them from the minor groove. This behavior is very interesting because allows, by means of a fine tuning on the isoxazolidine ring, to synthesize drugs that could bind DNA specifically to AT or GC nucleobases.

Further application of this template in antitumor agents design would seem warranted, particularly where systematic structural variations of the isoxazolidine nucleus are performed.

4. Experimental section

4.1. Chemistry

Melting points were determined with a Kofler apparatus and are uncorrected. Elemental analyses were performed with a Perkin–Elmer elemental analyzer. NMR spectra were recorded on a Varian instrument at 500 MHz (^{1}H) and at 125 MHz (^{13}C) using deuterochloroform or deuterobenzene as solvents; chemical shifts are given in ppm from TMS as internal standard. Thin-layer chromatographic separations were performed on Merck silica gel 60-F_{254} precoated aluminum plates. Preparative separations were carried out by flash chromatography using Merck silica gel 0.035–0.070 mm. Preparative centrifuge-accelerated radial thin-layer chromatography (PCAR-TLC) was performed with a Chromatotron® Model 7924T (Harrison Research, Palo Alto, CA, USA); the rotors (1 or 2 mm layer thickness) were coated with silica gel Merck grade type 7749, TLC grade, with binder and fluorescence indicator (Aldrich 34,644-6) and the eluting solvents were delivered by the pump at a flow-rate of 0.5–1.5 mL/min.

Analyses indicated by the symbols of the elements or functions were within 0.4% of the theoretical values.

PAH-aldehydes were purchased from Aldrich Co. All solvents were dried according to literature methods.

4.1.1. General procedure for the synthesis of isoxazolidines **4**–**7**

A solution of nitrone **3** (0.3 mmol) and *tert*-butyl-*N*-allylcarbamate or maleimide (0.45 mmol) in dry toluene (10 mL) in a sealed tube equipped with a stir bar, was allowed to react at 120 °C for 6 d or 18 h, respectively. The mixture was evaporated and the residue was purified by flash chromatography on a silica gel.

*4.1.1.1. tert-Butyl{[(3RS,5SR)-2-benzyl-3-(9-phenanthryl)isoxazolidin-5-yl]methyl}carbamate (**4a**).* Eluant ethyl acetate/cyclohexane 15:85 (second eluted product). Yield 53.3%, amorphous brownish solid. ^{1}H NMR ($CDCl_3$, 500 MHz): 1.16 (s, 9H), 2.04 (ddd, 1H, J = 6.3, 7.4 and 12.6 Hz, H_{4a}), 3.09 (ddd, 1H, J = 7.9, 8.3 and 12.6 Hz, H_{4b}), 3.26 (ddd, 1H, J = 2.3, 4.5 and 14.2 Hz, $H_{5'a}$), 3.32 (ddd, 1H, J = 4.5, 6.2 and 14.2 Hz, $H_{5'b}$), 3.94 (d, 1H, J = 14.3 Hz, $H_{2'a}$), 4.12 (d, 1H, J = 14.3 Hz, $H_{2'b}$), 4.44 (ddd, 1H, J = 2.3, 6.2, 6.3 and 8.3 Hz, H_5), 4.63 (dd, 1H, J = 7.4 and 7.9 Hz, H_3), 4.86 (t, 1H, J = 4.5 Hz, NH), 7.19–8.70 (m, 14H). ^{13}C NMR ($CDCl_3$, 125 MHz): 26.9, 28.4, 39.9, 43.2, 60.4, 66.5, 76.3, 122.4, 123.3, 124.0, 125.0, 126.1, 126.3, 126.4, 126.7, 127.3, 128.2, 128.9, 129.0, 130.3, 130.5, 131.1, 132.3, 156.3. Anal. $C_{30}H_{32}N_2O_3$ (C, H, N, O).

*4.1.1.2. tert-Butyl{[(3RS,5RS)-2-benzyl-3-(9-phenanthryl)isoxazolidin-5-yl]methyl}carbamate (**5a**).* Eluant ethyl acetate/cyclohexane 15:85 (first eluted product). Yield 26.7%, amorphous brownish solid. ^{1}H NMR ($CDCl_3$, 500 MHz): 1.42 (s, 9H), 2.39 (ddd, 1H, J = 6.8, 7.2 and 12.4 Hz, H_{4a}), 2.60 (ddd, 1H, J = 6.2, 8.2 and 12.4 Hz, H_{4b}), 3.32 (ddd, 1H, J = 4.3, 5.2 and 14.4 Hz, $H_{5'a}$), 3.38 (ddd, 1H, J = 2.8, 4.3 and 14.4 Hz, $H_{5'b}$), 3.82 (d, 1H, J = 14.2 Hz, $H_{2'a}$), 4.11

(d, 1H, $J = 14.2$ Hz, $H_{2'b}$), 4.31 (dddd, 1H, $J = 2.8$, 5.2, 6.2 and 7.2 Hz, H_5), 4.49 (dd, 1H, $J = 6.8$ and 8.2 Hz, H_3), 4.76 (t, 1H, $J = 4.3$ Hz, NH), 7.18–8.70 (m, 14H). ^{13}C NMR ($CDCl_3$, 125 MHz): 26.9, 28.1, 40.2, 43.7, 60.3, 66.2, 76.1, 122.4, 123.4, 123.8, 124.1, 126.3, 126.6, 126.8, 127.2, 128.4, 128.5, 128.9, 129.8, 129.9, 130.1, 131.2, 131.8, 156.1. Anal. $C_{30}H_{32}N_2O_3$ (C, H, N, O).

*4.1.1.3. tert-Butyl{[(3RS,5SR)-2-methyl-3-(pyren-1-yl)isoxazolidin-5-yl]methyl}carbamate (**4b**).* Eluant ethyl acetate/dichloromethane 7:83 (first eluted product). Yield 55.2%, amorphous yellow-brownish solid. ^{1}H NMR ($CDCl_3$, 500 MHz): 1.36 (s, 9H,), 2.18 (m, 1H, H_{4a}), 2.74 (s, 3H, *N*-Me), 3.13 (m, 1H, H_{4b}), 3.43 (m, 2H, $H_{5'}$), 4.52 (m, 1H, H_5), 4.69 (m, 1H, H_3), 5.21 (bs, 1H, NH), 7.99–8.33 (m, 9H). ^{13}C NMR ($CDCl_3$, 125 MHz): 28.3, 31.9, 43.7, 44.6, 69.2, 76.1, 122.2, 123.9, 124.8, 125.0, 125.3, 126.0, 126.8, 127.3, 127.4, 127.8, 128.6, 130.6, 131.3, 133.1, 156.1. Anal. $C_{26}H_{28}N_2O_3$ (C, H, N, O).

*4.1.1.4. tert-Butyl{[(3RS,5RS)-2-methyl-3-(pyren-1-yl)isoxazolidin-5-yl]methyl}carbamate (**5b**).* Eluant ethyl acetate/dichloromethane 7:83 (second eluted product). Yield 36.8%, amorphous yellow-brownish solid. ^{1}H NMR ($CDCl_3$, 500 MHz): 1.52 (s, 9H), 2.54 (m, 1H, H_{4a}), 2.72 (m, 4H, H_{4b} and *N*-Me), 3.42 (m, 1H, $H_{5'a}$), 3.56 (m, 1H, $H_{5'b}$), 4.50 (m, 1H, H_5), 4.56 (m, 1H, H_3), 5.06 (bs, 1H, NH), 7.99–8.42 (m, 9H). ^{13}C NMR ($CDCl_3$, 125 MHz): 28.4, 42.1, 43.5, 69.7, 76.4, 122.5, 124.4, 124.7, 124.9, 125.0, 125.2, 125.3, 125.9, 127.4, 127.7, 128.7, 130.59, 130.63, 131.3, 156.2. Anal. $C_{26}H_{28}N_2O_3$ (C, H, N, O).

*4.1.1.5. (3RS,3aRS,6aSR)-2-methyl-3-(pyren-1-yl)dihydro-2H-pyrrolo[3,4-d]isoxazole-4,6(3H,5H)-dione (**6b**).* Eluant ethyl acetate/cyclohexane 40:60 (second eluted product). Yield 69.6%, amorphous yellow-brownish solid. ^{1}H NMR ($CDCl_3$, 500 MHz): 2.81 (s, 3H, *N*-Me), 4.07 (dd, 1H, $J = 7.0$ and 9.0 Hz, H_{3a}), 4.89 (d, 1H, $J = 9.0$ Hz, H_{6a}), 5.00 (d, 1H, $J = 7.0$ Hz, H_3), 5.30 (s, 1H, *N*H), 8.00–8.24 (m, 9H). ^{13}C NMR ($CDCl_3$, 125 MHz): 42.9, 54.9, 71.3, 77.3, 121.3, 122.1, 123.5, 125.2, 125.4, 125.8, 126.1, 126.7, 127.5, 127.8, 128.6, 129.4, 130.6, 131.3, 151.1, 156.6. Anal. $C_{22}H_{16}N_2O_3$ (C, H, N, O).

*4.1.1.6. (3RS,3aSR,6aRS)-2-methyl-3-(pyren-1-yl)dihydro-2H-pyrrolo[3,4-d]isoxazole-4,6(3H,5H)-dione (**7b**).* Eluant ethyl acetate/cyclohexane 40:60 (first eluted product). Yield 17.4%, amorphous yellow ochre solid. ^{1}H NMR (CD_3COCD_3, 500 MHz): 4.16 (dd, 1H, $J = 4.5$ and 7.0 Hz, H_{3a}), 5.19 (d, 1H, $J = 7.0$ Hz, H_{6a}), 5.35 (d, 1H, $J = 4.5$ Hz, H_3), 8.06–8.72 (m, 9H), 10.46 (bs, 1H, NH). ^{13}C NMR (CD_3COCD_3, 125 MHz): 41.7, 50.3, 60.1, 79.3, 123.7, 125.4, 125.7, 125.9, 126.2, 126.4, 126.8, 127.1, 128.2, 128.5, 128.9, 131.5, 132.0, 132.2, 177.3. Anal. $C_{22}H_{16}N_2O_3$ (C, H, N, O).

*4.1.2. General procedure for the hydrolysis of cicloadducts **4** and **5***

To a solution of compound **4** or **5** (1 eq) in dry CH_2Cl_2 (10 mL) was added CF_3CO_2H (20.4 eq) at 0 °C. The reaction was raised to room temperature and magnetically stirred from 12 to 36 h. The reaction mixture was further neutralized with saturated $NaHCO_3$ (10 mL), and extracted with CH_2Cl_2 (3 × 10 mL); the reunited organic layers were anhydrified over Na_2SO_4 and the solvent evaporated at reduced pressure. The residue was purified by flash chromatography on a silica gel.

*4.1.2.1. 1-[(3RS,5SR)-2-Methyl-3-(pyren-1-yl)isoxazolidin-5-yl]methanamine (**8b**).* Eluant MeOH/CH_2Cl_2 1:9. Reaction time: 12 h. Yield 95%, amorphous yellow-brownish solid. ^{1}H NMR ($CDCl_3$, 500 MHz): 1.64 (bs, 2H, NH_2), 2.14 (m, 1H, H_{4a}), 2.77 (s, 3H, *N*-Me), 3.09 (m, 3H, H_{4b}, $H_{5'a}$ and $H_{5'b}$), 4.39 (m, 1H, H_5), 4.70 (m, 1H, H_3), 7.99–8.36 (m, 9H). ^{13}C NMR ($CDCl_3$, 125 MHz): 31.8, 42.7, 43.8, 69.3, 78.8, 122.3, 124.0, 124.8, 124.9, 125.0, 125.2, 125.9, 127.2, 127.4, 127.6, 128.5, 130.5, 130.6, 131.3. Anal. $C_{21}H_{20}N_2O$ (C, H, N, O).

*4.1.2.2. 1-[(3RS,5RS)-2-Methyl-3-(pyren-1-yl)isoxazolidin-5-yl]methanamine (**9b**).* Eluant MeOH/CH_2Cl_2 1:9. Reaction time: 36 h. Yield 80%, amorphous yellow-brownish solid. ^{1}H NMR ($CDCl_3$, 500 MHz): 1.63 (bs, 2H, NH_2), 2.53 (m, 1H, H_{4a}), 2.72 (m, 4H, H_{4b} and *N*-Me), 2.96 (m, 1H, $H_{5'a}$), 3.09 (m, 1H, $H_{5'b}$), 4.44 (m, 1H, H_5), 4.56 (m, 1H, H_3), 7.99–8.45 (m, 9H). ^{13}C NMR ($CDCl_3$, 125 MHz): 29.7, 43.8, 45.6, 69.9, 78.7, 122.6, 124.6, 124.8, 125.0, 125.1, 125.2, 125.3, 126.0, 127.3, 127.4, 127.7, 130.6, 130.7, 131.4. Anal. $C_{21}H_{20}N_2O$ (C, H, N, O).

*4.1.2.3. 1-[(3RS,5SR)-2-Benzyl-3-(9-phenanthryl)isoxazolidin-5-yl]methanamine (**8a**).* Eluant MeOH/CH_2Cl_2 1:9. Reaction time: 12 h. Yield 95%, amorphous brownish solid. ^{1}H NMR ($CDCl_3$, 500 MHz): 1.51 (bs, 2H, NH_2), 2.04 (m, 1H, H_{4a}), 2.78 (m, 1H, $H_{5'a}$), 3.04 (m, 1H, $H_{5'b}$), 3.14 (m, 1H, H_{4b}), 3.97 (d, 1H, $J = 14.5$ Hz, $H_{2'a}$), 4.21 (d, 1H, $J = 14.5$ Hz, $H_{2'b}$), 4.45 (m, 1H, H_5), 4.67 (t, 1H, $J = 7.5$ Hz, H_3), 7.28–8.80 (m, 14H). ^{13}C NMR ($CDCl_3$, 125 MHz): 41.1, 45.4, 60.4, 66.3, 77.1, 122.3, 122.4, 123.7, 124.2, 126.3, 126.6, 126.8, 127.2, 128.3, 128.5, 128.9, 129.8, 130.1, 130.8, 131.6, 134.3, 137.8. Anal. $C_{25}H_{24}N_2O$ (C, H, N, O).

*4.1.2.4. 1-[(3RS,5RS)-2-Benzyl-3-(9-phenanthryl)isoxazolidin-5-yl]methanamine (**9a**).* Eluant MeOH/CH_2Cl_2 1:9. Reaction time: 36 h. Yield 80%, amorphous brownish solid. ^{1}H NMR ($CDCl_3$, 500 MHz): 1.70 (bs, 2H, NH_2), 2.41 (m, 1H, H_{4a}), 2.63 (m, 1H, H_{4b}), 2.82 (dd, 1H, $J = 6.1$ and 13.2 Hz, $H_{5'a}$), 2.96 (dd, 1H, $J = 2.5$ and 13.2 Hz, $H_{5'b}$), 3.86 (d, 1H, $J = 14.8$ Hz, $H_{2'a}$), 4.12 (d, 1H, $J = 14.8$ Hz, $H_{2'b}$), 4.28 (m, 1H, H_5), 4.55 (m, 1H, H_3), 7.20–8.73 (m, 14H). ^{13}C NMR ($CDCl_3$, 125 MHz): 39.9, 45.2, 60.6, 66.8, 78.3, 122.3, 123.2, 124.1, 124.9, 126.3, 126.5, 126.6, 126.7, 127.0, 128.1, 128.8, 129.8, 130.2, 130.7, 131.5, 134.1, 137.7. Anal. $C_{25}H_{24}N_2O$ (C, H, N, O).

4.2. PM3 computational analysis

All the calculations were performed utilizing the PM3 [18] semiempirical hamiltonian as implemented in MOPAC 2009 package [24] using Winmostar as GUI interface [25]. In all the cases, full geometry optimization was carried out without any symmetry constraints with the keys precise, gnorm = 0.01 and ddmin = 0. Transition structures were found to have only one negative eigenvalue with the corresponding eigenvector involving the formation of the newly created C–C and C–O bonds.

4.3. Biological assay methods

4.3.1. Evaluation of cytotoxicity with MTS assay

Cytotoxicity of all compounds was evaluated by a commercial viability assay (CellTiter 96® Aqueous One Solution Assay, Promega Co., Madison WI), according to the Manufacturer's instructions. This assay is based on the principle that cells, at death, rapidly lose the ability to reduce MTS tetrazolium. Briefly, HeLa, MOLT-3, U-937, THP-1 and Vero cells were cultured in optimal culture conditions for 20 h in 96-well plates, in the absence of the compounds or in their presence, at concentrations ranging from 1 μM to 500 μM. At the end of the incubation time, the MTS tetrazolium-based reagent was added to each well. After a further incubation of 1 h at 37 °C in a humidified, 5% CO_2 atmosphere, the absorbance of the samples was recorded at 490 nm using a 96-well spectrophotometer. The assays were performed in triplicate. The inhibitory concentrations 50 (IC_{50}) were calculated as the concentrations of the compounds required to cause 50% reduction of absorbance values. For all compounds a non-linear regression analysis was used.

4.3.2. Evaluation of cytotoxicity with SRB assay

TCA-fixed cells were stained for 30 min with 0.4% (wt/vol) SRB dissolved in 1% acetic acid. At the end of the staining period, SRB was removed and cultures were quickly rinsed four times with 1% acetic acid to remove unbound dye. The acetic acid was poured directly into the culture wells from a beaker. Residual wash solution was removed by sharply flicking plates over a sink, which ensured the complete removal of rinsing solution. After being rinsed, the cultures were air dried until no standing moisture was visible. Bound dye was solubilized with 10 mM unbuffered Tris base (pH 10.5) for 5 min on a gyratory shaker.

OD was read in a UVmax microtiter plate reader (Molecular Devices, Menlo Park, CA). For maximum sensitivity, OD was measured at 564 nm.

4.3.3. ΦX174 RF I DNA unwinding assay

Reaction mixtures (10 μL final volume) contained 0.3 μg supercoiled ΦX174 RF I DNA in reaction buffer (10 mM Tris·HCl, pH 7.5, 50 mM KCl, 5 mM $MgCl_2$, 0.1 mM EDTA, and 15 μg/mL bovine serum albumin) and 2 units of Top1 [26]. Reactions were performed at 37 °C for 30 min with Top1 alone followed by incubation in the presence or absence of drug for another 30 min. The reactions were terminated by the addition of 0.5% SDS and 0.5 mg/mL proteinase K. Samples were incubated for 30 min at 50 °C. Next, 1.2 μL of 10× loading buffer (20% Ficol 400; 0.1 M Na_2EDTA, pH 8.0, 1.0% SDS, and 0.25% bromphenol blue) were added and reactions mixtures were loaded onto a 1% agarose gel made in 1× TBE buffer. Gels were run in 1× TBE containing 0.1% SDS. After electrophoresis, DNA bands were stained in 10 μg/mL of ethidium bromide and visualized by transillumination with ultraviolet light (300 nm).

4.3.4. UV titration with calf thymus DNA

Sonicated ct-DNA (phenol extracted, lyophilized, average size 2000 bases, range 200–6000 bases) was obtained from Pharmacia (Milan). Water was purified through a Millipore Milli-Q system. All experiments were conducted in 10^{-2} M phosphate buffer at pH 7.4, containing 0.1 M NaCl. The pH of solution was measured with a glass electrode. The concentrations of polynucleotide, in base pair, were determined by absorption spectroscopy, using the following molar extinction coefficient: 6600 M^{-1} cm^{-1} at 260 nm. Absorption spectra were recorded with a Beckman 650 DU spectrophotometer. All the spectra were corrected for the dilution resulting from addition of polynucleotide solutions to the solution of **8b**.

In order to obtain the binding constant, K_b, related to association complex we used the half-reciprocal plot of the absorption titration data, according to Eq. (1) [27]:

$$[P]_{bp}/(\varepsilon_A - \varepsilon_F) = [P]_{bp}/(\varepsilon_A - \varepsilon_F) + 1/K_b(\varepsilon_A - \varepsilon_F) \quad (1)$$

Here $[P]_{bp}$ is the concentration of the polynucleotide in base pairs, ϵ_A, ϵ_F and ϵ_B correspond to A_{obs}/[**8b**], the extinction coefficient for the free **8b** and the extinction coefficient for the totally bound form of **8b**, respectively. The K_B value was derived by the ratio of the slope to intercept of the linear plot.

4.4. Molecular docking

All poly-d$(AT)_2$ and poly-d$(GC)_2$ fragments were 3′- and 5′-endcapped with a phosphate group and the system configured as a fully anionic oligonucleotide. Subsequently, the geometry was fully minimized with a convergence criterion of 0.005 kcal/mol per Å, assigning a distance-dependent dielectric of 1.0, 1–4 scale factors of 0.833 for the electrostatic part and of 0.5 for the Van der waals one, and the nonbonded cutoff on off.

For fine docking with AutoDock 4.0 we used the following parameters: grid spacing = 0.375 Å, number of runs = 10, npts = 60 60 60, ga_num_evals = 20,000,000, ga_pop_size = 150 and ga_num_generations = 27,000. The graphical user interface AutoDockTools (1.5.4, R24) [28] was used for establishing the Autogrid points as well as visualization of docked ligand-nucleic acid structures.

Acknowledgments

This work was partially supported by CINMPIS and MIUR (PRIN). The authors thank Prof. Salvatore Sortino for UV spectroscopic measures.

References

[1] L.S. Lerman, Structural considerations in the interaction of deoxyribonucleic acid and acridines, J. Mol. Biol. 3 (1961) 18–30.
[2] R.M. Wadkins, D.E. Graves, Interactions of anilinoacridines with nucleic acids: effects of substituent modifications on DNA-binding properties, Biochemistry 25 (1986) 5902–5910.
[3] W.A. Denny, DNA-intercalating ligands as anti-cancer drugs: prospects for future design, Anticancer Drug Des. 19 (1980) 1101–1106.
[4] (a) J. Sartorius, H.-J. Schneider, Intercalation mechanisms with ds-DNA: binding modes and energy contributions with benzene, naphthalene, quinoline and indole derivatives including some antimalarials, J. Chem. Soc. Perkin Trans. (1997) 2319–2328;
(b) G.J. Atwell, C.D. Bos, B.C. Baguley, W.A. Denny, Potential antitumor agents. 56. 'Minimal' DNA-intercalating ligands as antitumor drugs: phenylquinoline-8-carboxamides, J. Med. Chem. 31 (1988) 1048–1052.
[5] (a) B.C. Baguley, W.A. Denny, G.J. Atwell, B.F. Cain, Potential antitumor agents. 35. Quantitative relationships between antitumor potency and DNA binding for 4′-(9-acridinylamino)methanesulfon-*m*-anisidide analogues, J. Med. Chem. 24 (1981) 520–525;
(b) W.R. Grove, C.L. Fortner, P.H. Wiernik, Review of amsacrine, an investigational antineoplastic agent, Clin. Pharm. 4 (1982) 320–326.
[6] G.J. Atwell, B.C. Baguley, G.J. Finlay, G.W. Rewcastle, W.A. Denny, Potential antitumor agents. 47. 3′-Methylamino analogs of amsacrine with in vivo solid tumor activity, J. Med. Chem. 29 (1986) 1769–1776.
[7] (a) R.E. Durand, Distribution and activity of antineoplastic drugs in a tumor model, J. Natl. Cancer Inst. 81 (1989) 146–152;
(b) T.J. Bichay, W.R. Inch, Resistance of V79 multicell spheroids to mitoxantrone: drug uptake and cytotoxicity, Cancer Drug Deliv. 4 (1987) 201–211;
(c) H. Liang, X. Wu, L.J. Guziec, F.S. Guziec Jr., K.K. Larson, J. Lang, J.C. Yalowich, B.B. Hasinoff, A structure-based 3D-QSAR study of anthrapyrazole analogues of the anticancer agents losoxantrone and piroxantrone, J. Chem. Inf. Model. 46 (2006) 1827–1835.
[8] (a) K.O. Hicks, S.J. Ohms, P.L. Van Zijl, W.A. Denny, P.J. Hunter, W.R. Wilson, An experimental and mathematical model for the extravascular transport of a DNA intercalator in tumours, Br. J. Cancer 76 (1997) 894–903;
(b) K.O. Hicks, F.B. Pruijn, B.C. Baguley, W.R. Wilson, Extravascular transport of the DNA intercalator and topoisomerase poison *N*-[2(dimethylamino) ethyl]acridine-4carboxamide (DACA): diffusion and metabolism in multicellular layers of tumor cells, J. Pharmacol. Exp. Ther. 297 (2001) 1088–1098.
[9] W.A. Denny, G.J. Atwell, B.C. Baguley, 'Minimal' DNA-intercalating agents as anti-tumour drugs: 2-styrylquinoline analogues of amsacrine, Anticancer Drug Des. 2 (1987) 263–270.
[10] (a) W.R. Wilson, W.A. Denny, in: W.C. Dewey, M. Edington, R.J.M. Fry, E.J. Hall, G.F. Whitmore (Eds.), Radiation Research: a 20th-Century Perspective, vol. 2, Academic Press, New York, 1992, pp. 796–801;
(b) E.I. Cussler, Diffusion and Mass Transfer in Fluid Systems. Cambridge University Press, Cambridge, 1984.
[11] A. Rescifina, M.A. Chiacchio, A. Corsaro, E. De Clercq, D. Iannazzo, A. Mastino, A. Piperno, G. Romeo, R. Romeo, V. Valveri, Synthesis and biological activity of isoxazolidinyl polycyclic aromatic hydrocarbons: potential DNA intercalators, J. Med. Chem. 49 (2006) 709–715.
[12] A. Rescifina, U. Chiacchio, A. Piperno, S. Sortino, Binding of a non-ionic pyrenylisoxazolidine derivative to double-stranded polynucleotides, New J. Chem. 30 (2006) 554–561.
[13] (a) S. Usha, I.M. Johnson, R. Malathi, Interaction of resveratrol and genistein with nucleic acids, J. Biochem. Mol. Biol. 38 (2005) 198–205;
(b) A. Favier, M. Blackledge, J.-P. Simorre, S. Crouzy, V. Dabouis, A. Gueiffier, D. Marion, J.-C. Debouzy, Solution structure of 2-(pyrido[1,2-e]purin-4-yl) amino-ethanol intercalated in the DNA duplex d$(CGATCG)_2$, Biochemistry 40 (2001) 8717–8726;
(c) L. von Szentpaly, I.L. Shamovksy, Molecular mechanics explanation for the stereochemical and shape selectivity of B-DNA for "bay-region" carcinogens, Mol. Pharmacol. 47 (1995) 624–629;

(d) W. Pohle, M. Bohl, J. Flemming, H. Boehlig, Subsidiary hydrogen bonding of intercalated anthraquinonic anticancer drugs to DNA phosphate, Biophys. Chem. 35 (1990) 213–226.
[14] (a) T. Kano, T. Hashimoto, K. Maruoka, Asymmetric 1,3-dipolar cycloaddition reaction of nitrones and acrolein with a bis-titanium catalyst as chiral lewis acid, J. Am. Chem. Soc. 127 (2005) 11926–11927;
(b) G. Desimoni, G. Faita, M. Mella, M. Boiocchi, In search of exo-selective catalysts for enantioselective 1,3-dipolar cycloaddition between acryloylox-azolidinone and diphenylnitrone, Eur. J. Org. Chem. (2005) 1020–1027.
[15] (a) J.J.P. Stewart, Optimization of parameters for semiempirical methods I. Method, J. Comput. Chem. 10 (1989) 209–220;
(b) J.J.P. Stewart, Optimization of parameters for semiempirical methods II. Applications, J. Comput. Chem. 10 (1989) 221–264.
[16] P. Skehan, R. Storeng, D. Scudiero, A. Monks, J. McMahon, D. Vistica, J.T. Warren, H. Bokesch, S. Kenney, M.R. Boyd, New colorimetric cytotoxicity assay for anticancer-drug screening, J. Natl. Cancer Inst. 82 (1990) 1107–1112.
[17] N. Watanabe, D.A. Dickinson, D.M. Krzywanski, K.E. Iles, H. Zhang, C.J. Venglarik, H.J. Forman, A549 subclones demonstrate heterogeneity in toxicological sensitivity and antioxidant profile, Am. J. Physiol. Lung Cell. Mol. Physiol. 283 (2002) 726–736.
[18] R.F. Pasternack, E.J. Gibbs, Porphyrin and metalloporphyrin interaction with nucleic acids. in: A. Sigel, H. Sigel (Eds.), Metal Ions in Biological Systems, vol. 33. Marcel Dekker Inc., New York, 1996, pp. 367–397.
[19] Hyperchem, Release 7.5, Hypercube Inc., Gainesville, FL, USA
[20] W.D. Cornell, P. Cieplak, C.I. Bayly, I.R. Gould, K.M. Merz Jr., D.M. Ferguson, D.C. Spellmeyer, T. Fox, J.W. Caldwell, P.A. Kollman, A second generation force field for the simulation of proteins, nucleic acids, and organic molecules, J. Am. Chem. Soc. 117 (1995) 5179–5197.
[21] O.A. Santos-Filho, J.D. Figueroa-Villar, M.T. Araujo, Molecular modeling of the interaction of trypanocide guanyl hydrazones with B-DNA, Biorg. Med. Chem. Lett. 7 (1997) 1797–1802.
[22] G.M. Morris, D.S. Goodsell, R.S. Halliday, R. Huey, W.E. Hart, R.K. Belew, A.J. Olson, Automated docking using a lamarckian genetic algorithm and an empirical binding free energy function, J. Comput. Chem. 19 (1998) 1639–1662.
[23] (a) P.A. Holt, J.B. Chaires, O. Trent, Molecular docking of intercalators and groove-binders to nucleic acids using autodock and surflex, J. Chem. Inf. Model. 48 (2008) 1602–1615;
(b) C. Detering, G. Varani, Validation of automated docking programs for docking and database screening against RNA drug targets, J. Med. Chem. 47 (2004) 4188–4201.
[24] J.J.P. Stewart, Computational Chemistry (Version 9.335W). MOPAC2009, Colorado Springs, CO, USA, 2009. http://OpenMOPAC.net.
[25] Norio Senda, 3D-Graphics Program for Molecular Modelling and Visualization of Quantum Chemical Calculations.http://winmostar.com/index_en.html.
[26] Y. Pommier, J.M. Covey, D. Kerrigan, J. Markovits, R. Pham, DNA unwinding and inhibition of mouse leukemia L1210 DNA topoisomerase I by intercalators, Nucleic Acids Res. 15 (1987) 6713–6731.
[27] A.M. Pyle, J.P. Rehmann, R. Meshoyer, C.V. Kumar, N.J. Turro, J.K. Barton, Mixed-ligand complexes of ruthenium(II): factors governing binding to DNA, J. Am. Chem. Soc. 111 (1988) 3051–3058.
[28] M.F. Sanner, Python: a programming language for software integration and development, J. Mol. Graph. Model. 17 (1999) 57–61.